

## Reactivity of the Hydrido/Nitrosyl Radical $\text{MHCl(NO)(CO)(P}^i\text{Pr}_3)_2$ , $M = \text{Ru, Os}$

Alexei V. Marchenko, Andrei N. Vedernikov, David F. Dye, Maren Pink, Jeffrey M. Zaleski,\* and Kenneth G. Caulton\*

Indiana University, Department of Chemistry, Bloomington, Indiana 47405

Received August 6, 2003

The reaction of equimolar NO with the 16 electron molecule  $\text{RuHCl(CO)L}_2$  ( $L = \text{P}^i\text{Pr}_3$ ) proceeds, via a radical adduct  $\text{RuHCl(CO)(NO)L}_2$ , onward to form  $\text{RuCl(NO)(CO)L}_2$  (X-ray structure determination) and  $\text{RuHCl(HNO)(CO)L}_2$ , in a 1:1 mole ratio. The HNO ligand, bound by N and trans to hydride, is rapidly degraded by excess NO. The osmium complex behaves analogously, but the adduct has a higher formation constant, permitting determination of its IR spectrum; both  $\text{MHCl(CO)(NO)L}_2$  radicals are characterized by EPR spectroscopy, and DFT calculations on the Ru system show it to have a “half-bent” Ru–N–O unit with the spin density mainly on nitrogen. DFT (PBE) energies rule out certain possible mechanistic steps for forming the two products. A survey of the literature leads to the hypothesis that NO should generally be considered as a (neutral) Lewis base (2-electron donor) when it binds to a 16 electron complex which is resistant to oxidation or reduction, and that the resulting N-centered radical has a M–N–O angle of  $\sim 140^\circ$ , which distinguishes it from  $\text{NO}^-$  (bent at  $<140^\circ$ ) and from  $\text{NO}^+$  ( $>170^\circ$ ).

### Introduction

The ways in which a formally 19 valence electron molecule responds to minimize the instability associated with this electron count are revealing. They reinforce the significance of the 18 electron rule, but they show unusual bonding and/or redox alternatives (isomers) and thus they can inform us about the reactivity consequences of a 19 valence electron count. The reactivity patterns of radical organometallic species are currently underdeveloped.<sup>1–6</sup>

For binary metal carbonyls, NO reacts to replace an even number of electrons by virtue of two NO replacing three conventional Lewis bases, often CO.<sup>7,8</sup> The reactions of NO with transition metal hydride complexes are not simple substitutions, and invariably lead to the “disappearance” of the hydrides, either to identifiable  $\text{H}_2$  product (when the reagent complex is a dihydride), or (for monohydrides) to an unspecified fate.<sup>7,8</sup> The latter occurs most often when a monohydride complex is involved. Since monohydride

complexes  $\text{HML}_n$  (generally 18 valence electrons) nearly always have an even electron count, any adduct  $\text{HM(NO)L}_q$  cannot have a 16 or 18 valence electron count. In the rare case of the hydride-alternative pure  $\sigma$  ligand  $\text{CH}_3$ ,  $\text{W(CH}_3)_6$  reacts with excess NO to give<sup>9</sup>  $(\eta^2\text{-MeN(NO)O})_2\text{WMe}_4$  so here an even electron count is achieved by adding two NO per methyl modified.

We study here one new aspect of this subject in that we bind one NO to a 16 electron, Ru(II) complex, but the reagent complex is a monohydride. The hydride ligand is always a reactive functionality, and here we find that it is destined to react by hydrogen atom transfer, since that redox chemistry is a way to move from radical intermediates to even-electron products, a path that conventional wisdom suggests should be thermodynamically favorable. This is found to offer a new synthesis of coordinated nitroxyl, HNO. The reason that this is an unprecedented route to an HNO ligand is that, in the past, the NO ligand has been installed on a metal first, and then, some form of H, either  $\text{H}^+_{10}$  or  $\text{H}^-$ ,<sup>11,12</sup> is furnished in a bimolecular reaction. We also contrast the NO reaction chemistry of  $\text{RuHCl(CO)L}_2$  with that of its osmium analogue, which lengthens the lifetime of one intermediate to permit its infrared spectral detection.

\* To whom correspondence should be addressed. E-mail: caulton@indiana.edu (K.G.C.); zaleski@indiana.edu (J.M.Z.).

- (1) Tyler, D. R. *Prog. Inorg. Chem.* **1988**, *36*, 125.
- (2) Tyler, D. R.; Mao, F. *Coord. Chem. Rev.* **1990**, *97*, 119.
- (3) Tyler, D. R. *Acc. Chem. Res.* **1991**, *24*(11), 325.
- (4) Schut, D. M.; Keana, K. J.; Tyler, D. R.; Rieger, P. H. *J. Am. Chem. Soc.* **1995**, *117*(35), 8939.
- (5) Braden, D. A.; Tyler, D. R. *J. Am. Chem. Soc.* **1998**, *120* (5), 942.
- (6) Braden, D. A.; Tyler, D. R. *Organometallics* **1998**, *17* (18), 4060.
- (7) Hayton, T. W.; Legzdins, P.; Sharp, W. B. *Chem. Rev.* **2002**, *102*, 935.
- (8) Richter-Addo, G. R.; Legzdins, P. Oxford University Press: New York, 1992.

- (9) Shortland, A. J.; Wilkinson, G. *J. Chem. Soc., Dalton Trans.* **1973**, 872.
- (10) Southern, J. S.; Green, M. T.; Hillhouse, G. L.; Guzei, I. A.; Rheingold, A. L. *Inorg. Chem.* **2001**, *40* (23), 6039.
- (11) Sellmann, D.; Blum, N.; Heinemann, F. W.; Hess, B. A. *Chem.—Eur. J.* **2001**, *7*, 1874.
- (12) Sellman, D.; Sutter, J. Z. *Anorg. Allg. Chem.* **2003**, *629*, 893.

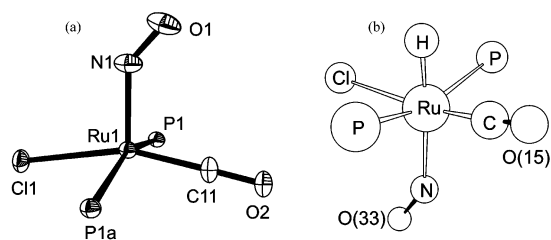


**Figure 1.** (a) ORTEP drawing (50% probability) of Ru(NO)Cl(CO)(P<sup>i</sup>-Pr<sub>3</sub>)<sub>2</sub> omitting alkyl carbons and attached hydrogen. (b) DFT-optimized geometry of RuHCl(NO)(CO)(P<sup>i</sup>Pr<sub>3</sub>)<sub>2</sub> with <sup>i</sup>Pr carbons and hydrogens omitted.

**Table 1.** Selected Bond Distances and Angles for RuCl(NO)(CO)(P<sup>i</sup>Pr<sub>3</sub>)<sub>2</sub>

Ru(1)	C(11)	1.7814(19)	
Ru(1)	N(1)	1.8566(11)	
Ru(1)	P(1)	2.4117(2)	
Ru(1)	Cl(1)	2.4905(5)	
C(11)	O(2)	1.149(2)	
N(1)	O(1)	1.1386(18)	
C(11)	Ru(1)	N(1)	98.92(7)
C(11)	Ru(1)	P(1)	89.32(7)
N(1)	Ru(1)	P(1)	100.448(5)
P(1)a	Ru(1)	P(1)	159.105(11)
C(11)	Ru(1)	Cl(1)	160.27(7)
N(1)	Ru(1)	Cl(1)	100.796(12)
P(1)a	Ru(1)	Cl(1)	89.715(13)
P(1)	Ru(1)	Cl(1)	86.391(13)
O(2)	C(11)	Ru(1)	172.9(2)
C(1)	P(1)	Ru(1)	111.76(3)
C(4)	P(1)	Ru(1)	114.35(3)
C(7)	P(1)	Ru(1)	112.31(3)
O(1)	N(1)	Ru(1)	138.75(11)

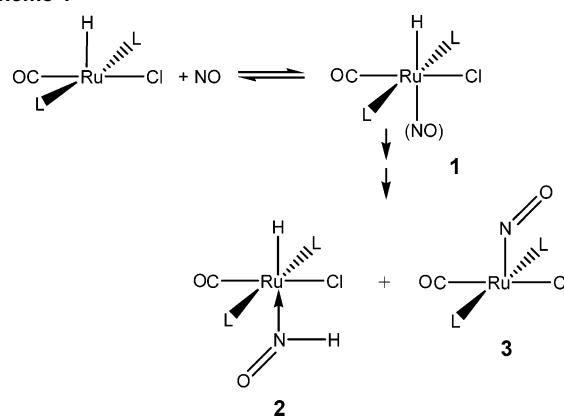
The results reported here fall into two distinct categories: (1) What is the nature of bonding and charge distribution when the odd electron species NO forms a 1:1 adduct with 16 valence electron species MHCl(CO)(P<sup>i</sup>Pr<sub>3</sub>)<sub>2</sub>? (2) How does the hydride play a role in the subsequent reaction chemistry of that adduct?<sup>13</sup>

## Results

The reaction of RuHCl(CO)L<sub>2</sub> with NO is one whose outcome depends critically on the presence or absence of free NO, and thus on the efficiency of mixing and on overall stoichiometry. An effective way to avoid excess NO, which we show below would take the primary product on to secondary products, is to employ a stoichiometry of less than one NO per Ru. In this way, and beginning at -70 °C in *d*<sub>8</sub>-toluene, one can see, by recording <sup>31</sup>P and <sup>1</sup>H NMR spectra, the production of essentially equimolar Ru(NO)Cl(CO)L<sub>2</sub> and RuHCl(HNO)(CO)L<sub>2</sub>.

If, in contrast, RuHCl(CO)L<sub>2</sub> (L = P<sup>i</sup>Pr<sub>3</sub>) is reacted with NO without exceptionally careful avoidance of excess NO, the product is Ru(NO)Cl(CO)L<sub>2</sub> alone. This square pyramidal (Figure 1a and Table 1) molecule has a bent NO in the apical coordination site and is thus isoelectronic with the hydride reagent. Apparently this structure is more stable than a saturated alternative with linear coordination of the nitrosyl. Despite the structural similarity to the hydride reagent, this product alone fails to account for the fate of the hydride ligand. As stated above, monitoring the reaction at lower tem-

## Scheme 1



perature is an effective way to clarify this point. These experiments, in *d*<sub>8</sub>-toluene beginning at -70°, show that, even at low temperature, the mole fraction conversion of RuHCl(CO)L<sub>2</sub> by substoichiometric NO (2:1 Ru to NO ratio) is only small, leading to slight broadening of the signals of RuHCl(CO)L<sub>2</sub>, but no NMR signals detectable for the 1:1 adduct (hence paramagnetic) RuHCl(NO)(CO)L<sub>2</sub>. Spectral monitoring, as the temperature is raised in 10° increments, shows growth of the equimolar diamagnetic products shown in Scheme 1.

While **3** is the product identified in the room temperature reaction in the presence of excess NO, **2** is new, and because it contains two hydrogens derived from RuHCl(CO)L<sub>2</sub>, it establishes material balance in the reaction. The most interesting spectral features of **2** are a hydride multiplet (triplet of doublets) and a resonance at 20.9 ppm characteristic of an HNO ligand.<sup>10</sup> At -20 °C, the coordinated HNO proton signal is a doublet, due to coupling with the hydride trans to itself. Compound **2** persists at 23 °C for more than 12 h provided the NO concentration is kept very low. When RuHCl(HNO)(CO)L<sub>2</sub> does slowly transform, due to even trace free NO, NMR and IR evidence shows HONO (+6.2 ppm, but variable, due to hydrogen bonding; 3642 cm<sup>-1</sup>) and N<sub>2</sub>O (2210 cm<sup>-1</sup>).

The nitroxyl group is sensitive to conversion, by excess free NO, as already established (eq 1).<sup>14,15</sup> Thus, when RuHCl(CO)L<sub>2</sub> is combined with excess NO even at -198 °C in *d*<sub>8</sub>-toluene, then slowly thawed and mixed, already at -60 °C there is essentially complete conversion to RuCl(NO)(CO)L<sub>2</sub> as the only metal complex product.



Additional evidence for the formation of the described products is obtained by using IR spectroscopy. When RuHCl(CO)(P<sup>i</sup>Pr<sub>3</sub>)<sub>2</sub> is reacted with NO in C<sub>6</sub>D<sub>6</sub>, the reaction mixture shows two sets of new bands, at 1911 and 1582 cm<sup>-1</sup>, attributed to  $\nu(\text{CO})$  and  $\nu(\text{NO})$  of Ru(NO)(CO)Cl(P<sup>i</sup>Pr<sub>3</sub>)<sub>2</sub> which are in good agreement with the previously reported data for the analogous complex Ru(NO)(CO)Cl(P<sup>i</sup>Bu<sub>2</sub>Me)<sub>2</sub><sup>16</sup> and at 1943 and 1392 cm<sup>-1</sup>, for RuH(HNO)(CO)Cl(P<sup>i</sup>Pr<sub>3</sub>)<sub>2</sub>. The in-

(13) Marchenko, A. V.; Vedernikov, A. N.; Dye, D. F.; Pink, M.; Zaleski, J. M.; Caulton, K. G. *Inorg. Chem.* **2002**, *41*, 4087.

(14) Bunte, S. W.; Rice, B. M.; Chabalowski, C. F. *J. Phys. Chem.* **1997**, *101*, 9430.

(15) Lee, T. J.; Dateo, C. E. *J. Chem. Phys.* **1995**, *103*, 9110.

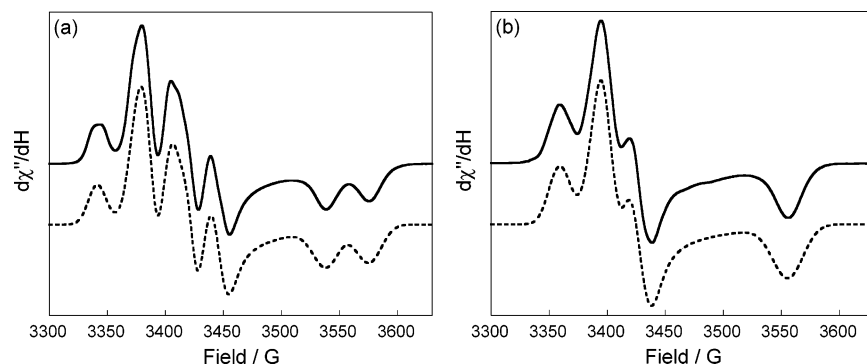


**Figure 2.** Observed (—) and calculated (---) X-band EPR spectra of  $\text{RuHCl(NO)(CO)(P}^i\text{Pr}_3)_2$  (a) and its RuD analogue (b) in toluene at 77 K.

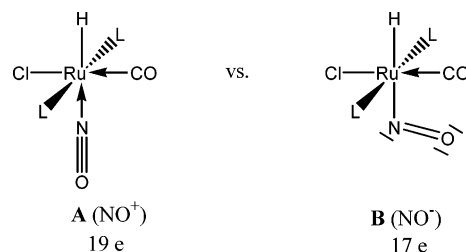
crease in  $\nu(\text{CO})$  for **3** in comparison to  $\text{RuHCl(CO)(P}^i\text{Pr}_3)_2$ ,  $1910\text{ cm}^{-1}$ , is due to a weaker donor power of the nitrosyl ligand in comparison to the hydride, and the higher  $\nu(\text{CO})$  and lower  $\nu(\text{NO})$  for the nitrosyl complex can be explained by the substantial back-donation from the metal to the nitrosyl ligand, and participation of  $\text{RuH(=N}^+\text{(H)—O}^-)(\text{CO})\text{Cl(P}^i\text{Pr}_3)_2$  resonance structure. Similar evidence for the  $\pi$ -accepting ability of the nitrosyl ligand and IR data has been reported recently.<sup>10</sup>

The X-ray structural study shows  $\text{RuCl(NO)(CO)L}_2$  (Figure 1a) to have a square pyramidal structure with an apical bent nitrosyl. It is therefore unsaturated and Ru(II) rather than the linear  $\text{RuNO}$  18 electron alternative, which would be Ru(0). All cis apical/basal angles are  $99^\circ \pm 1^\circ$ , and trans basal/basal angles are  $160^\circ \pm 1^\circ$ . The similarity of all Ru—P—C angles rules out any agostic interaction trans to the nitrosyl ligand. The NO group bends in the Cl—Ru—CO plane, although the disorder (crystallographic  $C_2$  symmetry along Ru1—N1) prevents knowing whether the nitrosyl O bends toward CO or toward Cl. The Ru—NO distance is longer (by  $0.075\text{ \AA}$  or  $25\sigma$ ) than the Ru—CO distance, consistent with a lower Ru—N bond order.

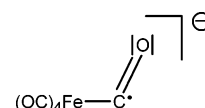
If **1** is indeed a good H-atom acceptor (to form **2**), it might be possible to intercept it with a H-atom donor, and thus divert the product from **3** (a hydrogen-loss product) toward **2**. Reaction of  $\text{RuHCl(CO)L}_2$  with NO (1:0.66 mole ratio) at  $20^\circ\text{C}$  in  $\text{C}_6\text{D}_6$ , in the presence of 20 equiv of 1,4-cyclohexadiene as a H atom donor, shows, within 5 min of combining the reagents, the formation of equimolar  $\text{RuHCl(HNO)(CO)L}_2$  and  $\text{RuCl(NO)(CO)L}_2$ , together with 25% unreacted  $\text{RuHCl(CO)L}_2$  (confirming the intended deficiency of NO); the yield of **2** is not enhanced. Under these conditions, it is thus impossible to trap any metal containing radical. The product distributions are the same even when the reaction is run in neat 1,4-cyclohexadiene. No products of any transformation (e.g., polymerization) of the diene were observed, thus indicating the highly selective reactivity of free radicals involved in this metal hydride chemistry. Further trapping experiments with the weaker Sn—H bond of  $(n\text{-Bu})_3\text{SnH}$  fail because this molecule reacts rapidly with  $\text{RuHCl(CO)L}_2$ .

On the surface, compound **1** might be considered as an analogue of 18 electron  $\text{RuHCl(CO)}_2\text{L}_2$ , but with one more electron, and one proton added to the carbon nucleus. It is thus a 19 valence electron complex (**A**) unless the nitrosyl

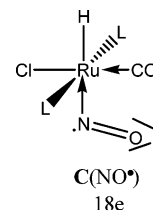
bends, in which case it is a 17 electron complex (**B**). Nineteen



electron complexes have been intensely studied among carbonyl complexes,<sup>1–6</sup> and the outcome is that the population of an M—ligand antibonding orbital is avoided by bending one MCO unit, and with radical character then residing primarily on that carbonyl. That carbonyl is then a one electron donor to the metal, so a 19 valence electron configuration at the metal is avoided. In effect, a metalla-



formyl radical is created. Another way to synthesize such a species is by binding CO to an odd electron complex, e.g.,  $\text{Rh}^{\text{II}}$  (porphyrin) + CO.<sup>17</sup> This additional option, in comparison to **A** and **B** above, permits the metal to achieve an 18 electron configuration, as in **C**. To the extent that the 18 electron rule truly semiquantitatively predicts reaction energies and “stability,” **C** may be the best representation of reality. We next review additional spectroscopic evidence.



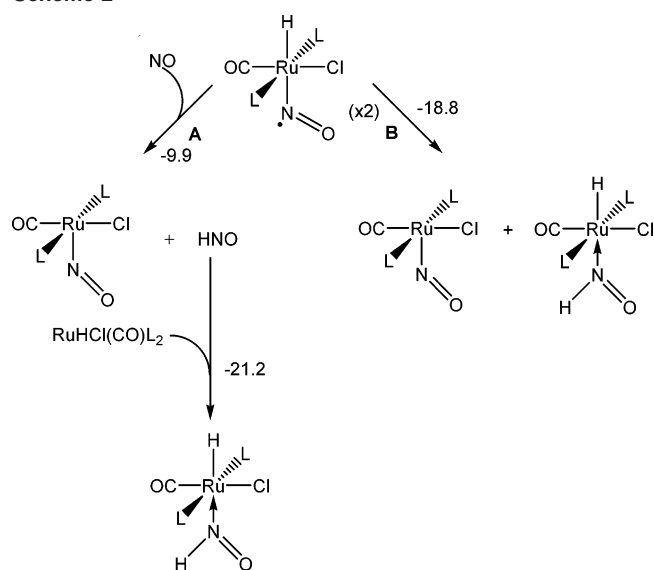
Under low temperature EPR conditions (77 K), the equilibrium position is shifted enough toward adduct that the (broad) EPR signal of free NO is not detected. The EPR spectrum of **1** (Figure 2a) reveals an  $S = 1/2$  spin system with near axial symmetry ( $g_x \approx g_y > g_z$ ) and simulated spin Hamiltonian parameters  $g_x = 2.006$ ,  $g_y = 1.993$ , and  $g_z = 1.910$  which were obtained using Monte Carlo methods.<sup>18</sup>

Strong nitrogen ( $I = 1$ , NO) hyperfine coupling ( $A_x^N = 34.5$  G) splits  $g_x$  into a 3-line pattern. Comparable superhyperfine coupling of the hydride ligand trans to the nitrogen further splits the three line pattern of  $g_x$  ( $A_x^H = 36.5$  G) as well as  $g_y$  ( $A_y^H = 35.1$ ) generating multiple overlapping signals which are responsible for the four line pattern observed at  $g \approx 2$ . Additional minor coupling of the electron spin to NO and resolved coupling to hydride are also observed on the remaining axes ( $A_y^N = 3.9$  G,  $A_z^N = 1.7$  G,  $A_z^H = 35.8$  G). The EPR spectrum of the deuteride analogue (Figure 2b) confirms these assignments as the newly refined  $g$ -values are conserved ( $g_x = 2.001$ ,  $g_y = 1.994$ , and  $g_z = 1.910$ ) and only strong coupling to NO is observed ( $A_x^N = 34.3$  G,  $A_y^N = 4.9$  G,  $A_z^N = 4.5$  G,  $A_x^D = 2.1$  G,  $A_y^D = 2.1$  G,  $A_z^D = 1.9$  G) since the ratio  $\gamma_D / \gamma_H = 0.15$  makes coupling to deuterium unresolved. The large nitrogen hyperfine coupling constants, low  $g$ -values relative to Ru(III) EPR signals,<sup>19</sup> and strong similarities of the spin Hamiltonian parameters to well characterized Ru–NO<sup>•</sup> species<sup>20–22</sup> confirm that the unpaired electron resides primarily on the NO ligand.

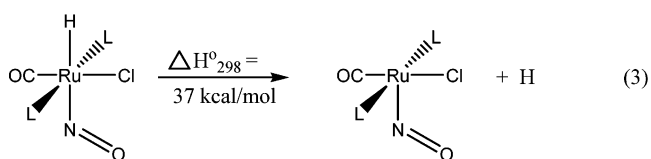
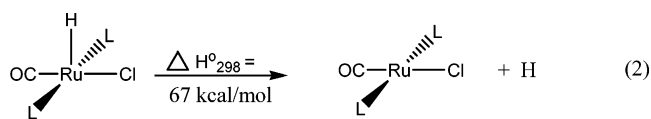
The observed reactivity of RuHCl(CO)L<sub>2</sub> toward NO appears to be relatively insensitive to the electron donating ability of the phosphine ligand L. When L = P<sup>i</sup>Pr<sub>3</sub> in RuHCl(CO)L<sub>2</sub> is replaced by a significantly less electron-donating phosphine P<sup>i</sup>Pr<sub>2</sub>(3,5-(CF<sub>3</sub>)<sub>2</sub>C<sub>6</sub>H<sub>3</sub>), and this complex<sup>23</sup> is combined with NO under the conditions of slight deficiency of NO, the NMR indicates the presence of RuCl(NO)(CO)-(P<sup>i</sup>Pr<sub>2</sub>(3,5-(CF<sub>3</sub>)<sub>2</sub>C<sub>6</sub>H<sub>3</sub>))<sub>2</sub> and RuHCl(HNO)(CO)(P<sup>i</sup>Pr<sub>2</sub>(3,5-(CF<sub>3</sub>)<sub>2</sub>C<sub>6</sub>H<sub>3</sub>))<sub>2</sub> in 1:1 ratio within 10 min after mixing.

**Mechanistic Insights from DFT Calculations.** The key event in the mechanism in Scheme 1 is H atom transfer from Ru to N. This is necessary to form a nonhydride product, and to eliminate odd-electron species. The rest are “merely” steps forming Ru–N bonds. DFT (PBE) reaction energies, calculated on a model with PMe<sub>3</sub> ligands, permit exclusion of certain homolytic elementary processes as being too endergonic to account for the observed rates.<sup>24,25</sup>

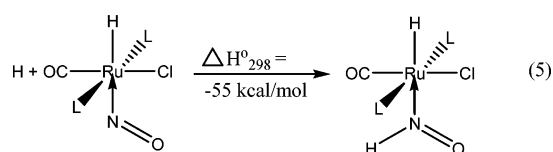
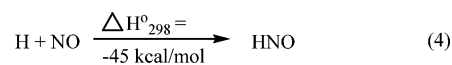
There are two different metal hydrides that are candidates for serving as the hydrogen atom donor. The reagent hydride complex is not a viable source for H-atom transfer (eq 2) because  $\Delta H^\circ_{298}$ , its bond dissociation enthalpy, is too large. The DFT energies (kcal/mol) of the two homolytic dissociations show the 19 electron radical (eq 3) to be the thermodynamically preferred H atom donor; this ranking

Scheme 2<sup>a</sup>

certainly rests on the greater stability of RuCl(NO)(CO)L<sub>2</sub> (eq 3), an observed product, than that of the unknown 15 valence electron radical RuCl(CO)L<sub>2</sub> (eq 2).



The two candidates to abstract a hydrogen atom are NO itself (eq 4) and RuHCl(NO)(CO)L<sub>2</sub> (eq 5), and the N–H bond formation energies of these two are similar, although H transfer to free NO is slightly less preferred at this level of calculation. Even at high computational levels,<sup>26,27</sup> the



N–H bond in free HNO was found to be very weak (43.6 kcal/mol<sup>27</sup>).

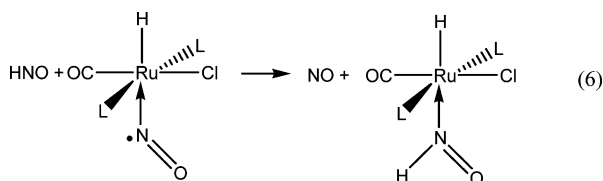
On the basis of these preliminaries, the two mechanisms in Scheme 2 (which shows standard free energies) can be evaluated.<sup>24,25</sup> Mechanism B is “direct” in that H-atom transfer between two identical metal complexes produces both observed products in a single step (i.e., a single bond rupture). Mechanism A has more steps, and ends with free HNO binding to available RuHCl(CO)(PMe<sub>3</sub>)<sub>2</sub> to form the second observed product. Alternatively, the HNO could serve

- (16) Ogasawara, M.; Huang, D.; Streib, W. E.; Huffman, J. C.; Gallego-Planas, N.; Maseras, F.; Eisenstein, O.; Caulton, K. G. *J. Am. Chem. Soc.* **1997**, *119*, 8642.
- (17) Wayland, B. B.; Sherry, A. E.; Bunn, A. G. *Inorg. Chem.* **1981**, *20*, 3093.
- (18) Neese, F. *QCPE Bull.* **1995**, *5*, 15.
- (19) Munshi, P.; Samanta, R.; Lahiri, G. K. *J. Organomet. Chem.* **1999**, *586*, 176.
- (20) Sellmann, D.; Gottschalk-Gaudig, T.; Haussinger, D.; Heinemann, F. W.; Hess, B. A. *Chem.—Eur. J.* **2001**, *7*, 2099.
- (21) McGarvey, B. R.; Ferro, A. A.; Tfouni, E.; Bezerra, C. W. B.; Bagatin, I.; Franco, D. W. *Inorg. Chem.* **2000**, *39*, 3577.
- (22) Wanner, M.; Scheiring, T.; Kaim, W.; Slep, L. D.; Baraldo, L. M.; Olabe, J. A.; Zalis, S.; Baerends, E. J. *Inorg. Chem.* **2001**, *40*, 5704.
- (23) Marchenko, A. V.; Huffman, J. C.; Valerga, P.; Jimenez Tenorio, M.; Puerta, M. C.; Caulton, K. G. *Inorg. Chem.* **2001**, *40*, 6444.
- (24) Koch, W.; Holthausen, M. C. *A Chemist's Guide to Density Functional Theory*; Wiley-VCH: Weinheim, 2001.

**Table 2.** Calculated (DFT) Vibrational Frequencies ( $\text{cm}^{-1}$ )

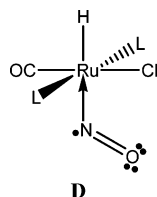
	$\text{RuCl(NO)(CO)(PMe}_3)_2$	$\xrightarrow[\text{a}]{+\text{H}^\bullet}$ $\text{RuHCl(NO)(CO)(PMe}_3)_2$	$\xrightarrow[\text{b}]{+\text{H}^\bullet}$ $\text{RuHCl(HNO)(CO)(PMe}_3)_2$
$\nu_{\text{CO}}$	1899	1941	1941
$\nu_{\text{Ru-H}}$	—	1852	1834
$\nu_{\text{NO}}$	1553	1670	1446

as an H-atom shuttle by transferring its  $\text{H}^\bullet$  (eq 6) to  $\text{RuHCl(NO)(CO)(PMe}_3)_2$  ( $\Delta H^\circ_{298} = -10$  kcal/mol).



However, the transition state for H-atom abstraction from  $\text{RuHCl(NO)(CO)L}_2$  will certainly have less steric repulsion when it is done by NO (**A**, Scheme 2) than by another molecule of  $\text{RuHCl(NO)(CO)L}_2$  (**B**, Scheme 2), thus favoring path **A**.

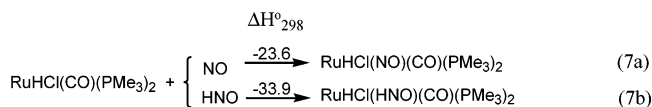
The structure of **1** was calculated (Figure 1b) by geometry optimization of the DFT (PBE) energy of the full  $\text{RuHCl(CO)(NO)(PiPr}_3)_2$  species. While it is certainly an octahedral structure around Ru, the interesting features are the long Ru–N bond (2.015 Å, long even compared to the Ru–N distance, 1.857(1) Å in  $\text{Ru(NO)(Cl)(CO)L}_2$ ), and the bend at N. The N/O distance, 1.187 Å, is longer than in free NO. Since the spin density on Ru is only 0.04 e, and the NO carries the other 0.87 e, the ground state of this adduct is truly a ligand-centered radical. A Lewis structure consistent with all of the above is **D**, which shows that adduct formation involves a 16 electron Ru achieving an 18 (not 19) electron configuration by localizing the extra electrons on oxygen (note the two lone pairs on oxygen). As a result, this N/O bond order



approximates 2, and the unpaired electron is localized heavily on N (although this is really derived from an N/O  $\pi^*$  orbital, so there is some radical character on oxygen also). Simple reasoning on degree of bonding versus occupancy of the lone “pair” orbital on N suggests that the Ru–N–O angle will be larger than the  $120^\circ$  of RNO when the nitrogen orbital is only half occupied, hence the  $143^\circ$  angle here. We suggest

that, in general, a  $\sim 140^\circ$   $\angle\text{M–N–O}$  should be taken as possible evidence for nitrogen-centered radical Lewis base behavior of neutral NO. There is good empirical evidence<sup>28</sup> that this is the case for NO bound to a variety of unsaturated  $d^6$  complexes (even when that yields only a 16 valence electron species).

**The Ru/N Bonds.** By the criterion of Ru–N bond dissociation enthalpy (BDE) of either NO (eq 7a) or HNO (eq 7b) toward  $\text{RuHCl(CO)(PMe}_3)_2$ , there is a difference between these two, but NO forms a satisfactory bond to  $\text{RuHCl(CO)(PMe}_3)_2$  despite the radical character of the product.



For comparison, the BDE of ammonia on the analogous species (eq 7c) is 7 kcal/mol. The low value for binding ammonia shows that, confronted with the trans effect of a hydride ligand, this pure  $\sigma$  donor forms only a very weak bond to  $\text{RuHCl(CO)L}_2$ .

**Trends in Vibrational Frequencies.** The calculated CO vibrational frequency stands as a useful gauge of  $\pi$ -basicity at the metal, and thus of concepts such as metal oxidation state. The three species involved in our reactivity studies are assembled in Table 2 in a way to illustrate their being related by formal hydrogen atom transfers. The  $\text{H}^\bullet$  in step **a** is added to the metal, and the rise in  $\nu_{\text{CO}}$  confirms that this is a net oxidation of the metal. The  $\text{H}^\bullet$  added in step **b** goes to nitrogen, and the constancy of  $\nu_{\text{CO}}$  in this step indicates that there is no significant redox change at the metal; more generally, the  $\pi$ -basicities of Ru in the presence of radical NO and of HNO are similar. The increase in the nitrosyl stretching frequency in step **a** is in agreement with a change  $\text{NO}^- \rightarrow \text{NO}^\bullet$  as Ru is oxidized, since the NO bond order increases from free diatomic  $\text{NO}^-$  to  $\text{NO}^\bullet$ . In step **b**, hydrogenation of coordinated  $\text{NO}^\bullet$  reduces the NO bond order to ca. 2.

**The Osmium Analogue.** The reaction of NO with  $\text{OsHCl(CO)L}_2$  ( $\text{L} = \text{P}^i\text{Pr}_3$ ) in benzene shows general similarities to the Ru analogue, but with quantitative differences. Under only 80 mm NO (0.5 mol/mol Os) in benzene at  $23^\circ\text{C}$ , there is essentially complete (stoichiometrically limited) formation of  $\text{OsHCl(NO)(CO)L}_2$ , which causes complete loss of the

(25) Cramer, C. J. *Essentials of Computational Chemistry: Theories and Models*; J. Wiley: West Sussex, England, 2002.

(26) Tschumper, G. S.; Schaefer, H. F., III. *J. Chem. Phys.* **1997**, *107*, 2529.

(27) Mordaunt, D. H.; Flothmann, H.; Stumpf, M.; Keller, H.-M.; Beck, C.; Schinke, R.; Yamashita, K. *J. Chem. Phys.* **1997**, *107*, 6603.

(28) Scheidt, W. R.; Ellison, M. K. *Acc. Chem. Res.* **1999**, *32*, 350.

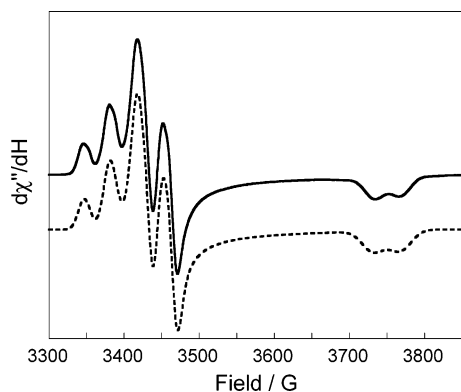


**Figure 3.** Observed (—) and calculated (---) X-band EPR spectra of  $\text{OsHCl(NO)(CO)(P}^i\text{Pr}_3)_2$  in toluene at 77 K:  $g_x = 1.998$ ,  $g_y = 1.974$ ,  $g_z = 1.812$ ,  $A_x^N = 35.9$  G,  $A_y^N = 5.1$  G,  $A_z^N = 2.5$  G,  $A_x^H = 32.0$  G,  $A_y^H = 30.7$  G,  $A_z^H = 32.7$  G.

$^1\text{H}$  NMR signals in the normal position of those of  $\text{OsHCl(CO)L}_2$ , as well as complete loss of  $^{31}\text{P}$   $\{^1\text{H}\}$  NMR signals. This higher equilibrium concentration of NO adduct is consistent with the generally higher adduct formation constant for Os versus Ru for nonradical Lewis bases. There is also a weak and broad  $^1\text{H}$  NMR peak at 4.0 ppm attributed to HONO. Upon addition of 1 atm (i.e., excess) NO to this solution,  $^1\text{H}$  and  $^{31}\text{P}\{^1\text{H}\}$  NMR spectra taken within 15 min show  $\text{OsHCl(HNO)(CO)L}_2$  and  $\text{OsCl(NO)(CO)L}_2$ <sup>29</sup> in a 1:4 mole ratio as the major products. The 4.0 ppm HONO peak is now stronger and broader. The peak due to coordinated nitroxyl is far downfield, 20.9 ppm, and is a doublet with coupling identical to the coupling in the triplet of doublets pattern due to hydride at  $-8.38$  ppm; this identical doublet coupling proves that these protons are both in the same molecule and that there is only one of each type. Thus, a nitroxyl ligand is also produced in the osmium case, and it is subject to degradation by excess NO, but much more slowly than in the case of ruthenium.

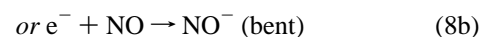
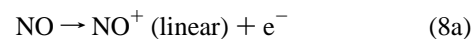
In this osmium system, the reaction of H atom abstraction is slower, and the initially formed radical  $\text{OsH(NO}\cdot\text{)(CO)Cl(P}^i\text{Pr}_3)_2$  is present in higher mole fraction, even with substoichiometric NO, at  $-60$  °C. The radical complex is therefore detectable by IR spectroscopy with  $\nu(\text{CO})$  at  $1903$   $\text{cm}^{-1}$  and  $\nu(\text{NO})$  at  $1559$   $\text{cm}^{-1}$ . The increase in  $\nu(\text{CO})$  from  $\text{OsHCl(CO)(P}^i\text{Pr}_3)_2$  ( $1888$   $\text{cm}^{-1}$ ) to its NO adduct is explained by back-donation from the Os center to the NO ligand; this also explains the longer life of this radical in the case of Os since it is more reducing than Ru. Upon addition of a larger amount of NO to the reaction mixture, the formation of  $\text{OsCl(NO)(CO)(P}^i\text{Pr}_3)_2$  and  $\text{OsH(HNO)(CO)Cl(P}^i\text{Pr}_3)_2$  is confirmed by the appearance of  $\nu(\text{CO})$  and  $\nu(\text{NO})$  of these products at  $1892$  and  $1552$   $\text{cm}^{-1}$  for the nitrosyl complex, and at  $1929$  and  $1388$   $\text{cm}^{-1}$  for the nitroxyl complex. These values are lower than for the analogous Ru products due to the higher extent of the back-donation from more reducing Os to CO, NO, and (HNO) ligands.

The EPR spectrum of  $\text{OsHCl(NO)(CO)L}_2$  in a frozen glass at 77 K (Figure 3) is generally similar in shape to that of

the Ru analogue, but with a greater separation of the  $g_z$  from the  $g_x$  and  $g_y$  values. The superhyperfine parameters are analogous to those for the Ru analogue, and as for Ru, any coupling to P was unresolvable. Noteworthy is the significant coupling to hydrogen, which has only a  $\sigma$  orbital. This is useful experimental evidence that the SOMO cannot have  $\pi^*(\text{NO})$  character (i.e., perpendicular to the MNO plane), since that does not have the symmetry to mix with the hydrogen orbital. The half filled N ( $sp^2$ ) orbital does have symmetry to mix with a metal orbital and the H (1s) orbital, to give the observed  $A^H$  coupling. The calculated spin densities for the model  $\text{MHCl(NO)(CO)(PMe}_3)_2$  help account for the observed superhyperfine coupling to the hydride ligand. Thus, although the spin densities are mainly (Ru/Os values given) on N (0.56/0.55), O (0.31/0.32), and M (0.04/0.04), there is nonzero hydride participation in the SOMO such that the hydride populations are 0.09 and 0.08. While there is some unpaired spin on the metals, it is less than that on the hydride, and the radical character at hydride is a reminder that hydrogen atom transfer becomes an attractive mode of reactivity. This is also why the Ru–H BDE (eq 3) is so low. It must be recognized that the nonzero  $A^H$  value to hydride is direct evidence that the Ru–N–O unit is nonlinear, since only then does the H 1s orbital mix with nitrogen orbitals in the SOMO.

## Discussion

The collective results presented here show that  $\text{MHCl(CO)L}_2$  (M = Ru, Os) is neither readily oxidizable nor reducible by NO, thus frustrating one NO molecule from behaving in its “typical” way upon encountering a metal (eq 8a,b).



The dominant reactivity of unsaturated  $\text{MHCl(CO)L}_2$  is to find a conventional Lewis base, and it is in this way that NO is forced to act, despite thus creating a diatomic ligand-centered radical. Indeed, it has been concluded recently,<sup>30</sup> for  $d^6$  metals, “NO behaves as a normal nucleophile in ligand substitution reactions...even though it is a radical.”

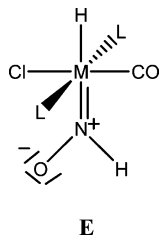
A recent report shows how the reactivity shown in eq 8b can lead to porphyrin ligand oxidation, which is then manifest as C–C bond formation to a second porphyrin complex.<sup>31</sup>

The hydride chemical shift of  $\text{RuHCl(HNO)(CO)L}_2$  is sufficiently far downfield from that of  $\text{RuHCl(CO)L}_2$  that it indicates a “strong” ligand trans to itself. The nitroxyl proton chemical shift is also very far downfield at 20 °C, suggesting some strong influence by the metal (e.g., anisotropic deshielding). Taken together, and arguing as we have earlier about

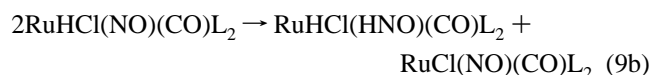
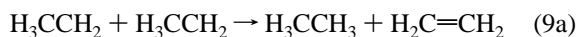
(29) Renkema, K. B.; Caulton, K. G. *New J. Chem.* **1999**, *23*, 1027.

(30) Wolak, M.; van Eldik, R. *Coord. Chem. Rev.* **2002**, *230*, 263–282.  
(31) Rath, S. P.; Koerner, R.; Olmstead, M. M.; Balch, A. L. *J. Am. Chem. Soc.* **2003**, *125*, 11798.

carbene complexes<sup>32</sup> and about vinyl complexes,<sup>33,34</sup> participation by resonance form **E** is suggested. Note that the  $\nu_{NO}$  value for the osmium nitrosyl complex,  $1388\text{ cm}^{-1}$ , is close to the value for N/O single bonds, consistent with Os being a stronger  $\pi$  acid than Ru.



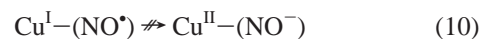
The net conversion of two 19 electron radical hydrides is in some ways analogous to that of two ethyl radicals to give an alkane and an olefin (eq 9). Both are *net* H-atom transfers, or disproportionation.



The (probable) mechanistic difference is that eq 9b, for steric reasons, does not occur by a step bimolecular in Ru, but instead requires free NO as a sterically compact H atom “shuttle,” and the weak H–Ru bond in  $RuHCl(NO)(CO)L_2$  facilitates this shuttle role. The weak H–N bond in HNO leads to its final destruction by excess NO.

**Comparison to Other Nitrosyls.** A closely analogous situation was reported for the  $d^{10}$ , 16 electron reagent  $Tp^{R,R'}Cu^I$ , incorporating various tris-pyrazolylborate ligands.<sup>35,36</sup> These bind one NO, incompletely at 1 atm and  $25\text{ }^\circ\text{C}$ , to give the adducts  $Tp^{R,R'}Cu(NO)$  which spectroscopic and crystallographic studies reveal to have  $\eta^3$ -Tp and a bent ( $\angle Cu-NO = 163.4^\circ$ ) nitrosyl. EPR studies show large ( $\sim 30$  G) hyperfine coupling to N (and also to copper), and  $g$  values significantly different from those of  $TpCu^{II}N_3$ . These “electron excess” metal complexes (19 valence electrons if three electrons of NO are counted) were concluded to be best represented as  $Cu^I(NO^\bullet)$  oxidation levels. Clearly all of this is an unsaturated  $d^{10} + NO$  analogue of our unsaturated  $d^6 + NO$  chemistry. Moreover, the single crystal structure of a  $Tp^{R,R'}CuNO$  species shows large anisotropic thermal ellipsoids for the nitrosyl oxygen, indicative perhaps of disorder, and so the reported  $\angle Cu-N-O$  may be in error. Since the  $163.4^\circ$  angle was fixed in the quantum calculations, geometry optimization by more modern methods may show an even smaller angle, as found here in  $RuHCl(NO)(CO)L_2$ . In sum, this seems to be another d electron configuration

where intramolecular redox transfer (eq 10) is not favored, and NO binds as a “simple” Lewis base, but with a nonlinear Cu–N–O geometry.



An earlier example of addition of NO to a 16 electron molecule involves  $RhCl(\text{porphyrin})$ .<sup>37</sup>

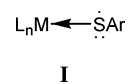
It has been previously established from spectroscopic studies that  $Ru(NO)(NH_3)_5^{2+}$ ,<sup>38</sup>  $Ru(NO)Cl(\text{bipy})_2^+$ ,<sup>39,40</sup> and  $CpRh(NO)(PR_3)_4^+$  are all bent nitrosyls with considerable spin density on N. In the case of  $CpCr(NO)_2(PR_3)$ , the radical character appears to be delocalized over two nitrosyls, and no significant CrNO bending is evident in the crystal structure.<sup>42</sup> In the case of  $M(NO)_2(\text{porphyrin})$ , where  $M = Fe$  or  $Ru$ , both nitrosyls bend.<sup>17,28</sup> Only in the case of  $Ru(NO)(NH_3)_5^{2+}$  was free radical reactivity described, and the product of reaction with added  $R^\bullet$  was stated to be coordinated  $RNO$ .<sup>38</sup>

The units (tetradentate)( $FeNO^{2+}$ ) have been further characterized<sup>43</sup> as having low spin  $d^6$   $Fe^{II}$  with coordinated  $NO^\bullet$  radical, further complicated by coexistence of a second spin state; such spin-equilibrium behavior is most frequent for 3d metals, but not for the 4d and 5d metals studied here.

**Comparison to Other Ligand-Centered Radicals.** We point out that **F**, **G**, and **H** are analogous to the  $MHCl(CO)(NO)L_2$  species reported here in being the product of bonding a radical ( $PhS^\bullet$  or  $I^\bullet$ ) to a 16 electron fragment.



While the metal oxidation state of each of these is represented in the literature<sup>44–46</sup> assuming anionic SPh and I (thus  $Mn^{II}$  and  $W^I$ ), each may to varying extents involve ligand-centered radicals. For SAr especially, the bonding could be represented as **I**, which is to say that  $Mn^I$  and  $W^0$ , in the ligand environment, are not oxidized by the radicals I or ArS.



Indeed, the EPR  $g$  values of species **F**,  $1.977 \rightarrow 2.068$ , are close enough together to suggest major light atom participation in the SOMO, but certainly with some metal character (manganese hyperfine structure is resolved). The similarity here is that both the NO adducts reported here and **F–H** involve the interaction of a  $d^6$  metal fragment with a radical which also has lone pairs on the coordinating atom.

(32) Huang, D.; Spivak, G. J.; Caulton, K. G. *New J. Chem.* **1998**, 22 (10), 1023.

(33) Marchenko, A. V.; Gerard, H.; Eisenstein, O.; Caulton, K. G. *New J. Chem.* **2001**, 25 (10), 1244.

(34) Caulton, K. G. *J. Org. Chem.* **2001**, 617, 56.

(35) Schneider, J. L.; Carrier, S. M.; Ruggiero, C. E.; Young, V. G., Jr.; Tolman, W. B. *J. Am. Chem. Soc.* **1998**, 120, 11408.

(36) Ruggiero, C. E.; Carrier, S. M.; Antholine, W. E.; Whittaker, J. W.; Cramer, C. J.; Tolman, W. B. *J. Am. Chem. Soc.* **1993**, 115, 11285.

(37) Wayland, B. B.; Newman, A. R. *Inorg. Chem.* **1981**, 20, 3093.

(38) Armor, J. N.; Hoffman, M. Z. *Inorg. Chem.* **1975**, 4, 444.

(39) Callahan, R. W.; Meyer, T. J. *Inorg. Chem.* **1977**, 16, 574.

(40) Callahan, R. W.; Brown, G. M.; Meyer, T. J. *J. Am. Chem. Soc.* **1975**, 97, 894.

(41) Geiger, W. E.; Rieger, P. H.; Tulyathan, B.; Rausch, M. D. *J. Am. Chem. Soc.* **1984**, 106, 7000.

(42) Yu, Y. S.; Jacobson, R. A.; Angelici, R. J. *Inorg. Chem.* **1982**, 21, 3106.

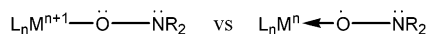
(43) Li, M.; Bonnet, D.; Eckhard, B.; Neese, F.; Weyhermueller, T.; Blum, N.; Sellmann, D.; Wieghardt, K. *Inorg. Chem.* **2002**, 41, 3444–3456.

In each case, a potential (but weak) oxidant encounters a metal/ligand fragment which is only weakly reducing.



A similar conclusion holds for the binding of the phenoxy group to a number of transition metals.<sup>47–51</sup> For chromium, manganese, iron, cobalt, and zinc, oxidation of the MOPh group beyond a certain level occurs primarily at the ligand, yielding a metal-coordinated phenoxy radical. The same is true for the unit  $\text{CuOPh}^{2+}$ , which is established to be  $\text{Cu}^{\text{II}}$  and a coordinated phenoxy radical, a situation which has been implicated in the function of galactose oxidase.<sup>52,53</sup>

Another class of potentially oxidizing radicals is the nitroxides,  $\text{R}_2\text{NO}$ . Since these are quite “stable” radicals, the rarer case is when they are themselves reduced to their monoanion,<sup>54</sup> and the more common cases are those (generally involving 3d metal ions) where they persist as ligand-localized radicals upon coordination.<sup>55,56</sup>



## Conclusions

This work shows the following: (1) The radical adducts  $\text{MHCl}(\text{NO})(\text{CO})\text{L}_2$  ( $\text{M} = \text{Ru}, \text{Os}$ ) are persistent. This adduct makes full utilization of the metal valence orbitals (i.e. 18 electron configuration), and the radical character is best borne by the NO ligand, especially at nitrogen. Thus, the radical character being borne by light atoms is analogous to nitroxide,  $\text{R}_2\text{NO}$ . (2) The adduct next confronts the problem that the two reactive functionalities, coordinated H and NO, are mutually trans in a nonfluxional species. This leaves the adduct metastable, at least with respect to intramolecular reactions. Bimolecular reactions thus become viable. (3) The radical appears to react further only with additional radical NO, and does so by H-atom transfer. This is especially

favorable because, following H atom abstraction from Ru or Os, the nitrosyl ligand can undergo intramolecular electron transfer from M to neutral radical NO, to give bent  $\text{NO}^-$ , in  $\text{M}(\text{NO})\text{Cl}(\text{CO})\text{L}_2$ . That is, the thermodynamics of H atom transfer become especially favorable because of the stability of the metal complex product. (4) The hydride hydrogen is fated to become part of light atom products because HNO reacts further, when additional NO is present, according to known metal-free reactions.

## Experimental Section

**General Considerations.** All manipulations were carried out using standard Schlenk and glovebox techniques under prepurified argon. All solvents were dried and distilled over appropriate agents and stored in airtight solvent bulbs with Teflon closures under argon prior to use. Nitrogen monoxide (Aldrich) and deuterium gas (Cambridge Isotope Laboratories) were used as received.  $\text{RuHCl}(\text{CO})(\text{P}^i\text{Pr}_3)_2$ <sup>57</sup> was prepared according to a previously reported procedures. <sup>1</sup>H (referenced to residual solvent impurity), <sup>2</sup>H, and <sup>31</sup>P (referenced to 85%  $\text{H}_3\text{PO}_4$ ) NMR spectra were collected on Varian Gemini 2000 (300 MHz <sup>1</sup>H, 121 MHz <sup>31</sup>P) and Varian Inova (400 MHz <sup>1</sup>H, 73 MHz <sup>2</sup>H) spectrometers. Infrared spectra were recorded on Nicolet 510P FT-IR and React-IR spectrometers. EPR spectra were obtained on a Bruker 300ESP spectrometer operating at X-band (~9.5 GHz): microwave power, 20 mW; modulation amplitude, 5.0 G, modulation frequency, 100 kHz; receiver gain,  $1.25 \times 10^4$ . All EPR spectra were observed in toluene as frozen glasses at 77 K. The values of unresolved coupling ( $A < 5.2$  G) are derived from the fitting program and are thus less accurate.

**Computations.** Geometry optimization, frequency analysis, calculations of energy, and Mulliken spin population in this work have been performed using density functional theory (DFT) method,<sup>58</sup> specifically functional PBE,<sup>59</sup> implemented in an original program package “Priroda”.<sup>60,61</sup> In PBE calculations, relativistic Stevens–Basch–Krauss (SBK) effective core potentials (ECPs)<sup>62–64</sup> optimized for DFT calculations have been used. The basis set was 311-split for main group elements with one additional polarization p-function for hydrogen, and an additional two polarization d-functions for elements of higher periods. Full geometry optimization was performed without constraints on symmetry. For all species under investigation, frequency analysis has been carried out. All minima have been checked for the absence of imaginary frequencies. Calculated IR frequencies were not scaled.

**Reaction of  $\text{RuHCl}(\text{CO})(\text{P}^i\text{Pr}_3)_2$  with Excess NO.** A solution of 13 mg (0.027 mmol) of  $\text{RuHCl}(\text{CO})(\text{P}^i\text{Pr}_3)_2$  in 0.5 mL of  $\text{C}_6\text{D}_6$  was placed in an NMR tube fitted with a Teflon stopcock. The solution was freeze–pump–thaw–degassed 3 times in liquid  $\text{N}_2$ , the headspace evacuated, and 1 atm NO (0.1 mmol) was introduced into the tube. The color of the solution became orange from yellow-orange. After stirring for 10 min at 23 °C, <sup>1</sup>H and <sup>31</sup>P{<sup>1</sup>H} NMR showed complete conversion of  $\text{RuHCl}(\text{CO})(\text{P}^i\text{Pr}_3)_2$  to  $\text{Ru}(\text{NO})\text{Cl}$ –

(44) Lang, R. F.; Ju, T. D.; Kiss, G.; Hoff, C. D.; Bryan, J. C.; Kubas, G. *J. Inorg. Chim. Acta* **1997**, *259*, 317.

(45) Lau, P.; Braunwarth, H.; Huttner, G.; Guenauer, D.; Evertz, K.; Imhof, W.; Emmerich, C.; Zsolnai, L. *Organometallics* **1991**, *10*, 3861.

(46) Milukov, V. A.; Sinyashin, O. G.; Ginzburg, A. G.; Kondratenko, M. A.; Loim, N. M.; Gubskaya, V. P.; Musin, R. Z.; Morozov, V. I.; Batyeva, E. S. *J. Org. Chem.* **1995**, *493*, 221.

(47) Bill, E.; Mueller, J.; Weyhermueller, T.; Wieghardt, K. *Inorg. Chem.* **1999**, *38*, 5795–5802.

(48) Chaudhuri, P.; Hess, M.; Mueller, J.; Hildenbrand, K.; Bill, E.; Weyhermueller, T.; Wieghardt, K. *J. Am. Chem. Soc.* **1999**, *121*, 9599–9610.

(49) Sokolowski, A.; Mueller, J.; Weyhermueller, T.; Schnepf, R.; Hildenbrandt, P.; Hildenbrand, K.; Bothe, E.; Wieghardt, K. *J. Am. Chem. Soc.* **1997**, *119*, 8889–8900.

(50) Sokolowski, A.; Adam, B.; Weyhermueller, T.; Kikuchi, A.; Hildenbrand, K.; Schnepf, R.; Hildenbrandt, P.; Bill, E.; Wieghardt, K. *Inorg. Chem.* **1997**, *36*, 3702–3710.

(51) Sokolowski, A.; Bothe, E.; Bill, E.; Weyhermueller, T.; Wieghardt, K. *Chem. Commun.* **1996**, *14*, 1671–1672.

(52) Jazdzewski, B. A.; Tolman, W. B. *Coord. Chem. Rev.* **2000**, *200*–202, 633–685.

(53) Halfen, J. A.; Young, V. G., Jr.; Tolman, W. B. *Angew. Chem., Int. Ed.* **1996**, *35*, 1687–1690.

(54) Evans, W. J.; Perotti, J. M.; Doedens, R. J.; Ziller, J. W. *Chem. Commun.* **2001**, 2326.

(55) Kahn, M. L.; Sutter, J.-P.; Golhen, S.; Guionneau, P.; Ouahab, L.; Kahn, O.; Chasseau, D. *J. Am. Chem. Soc.* **2000**, *122*, 3413.

(56) Ishii, K.; Fujisawa, J.-I.; Adachi, A.; Yamauchi, S.; Kobayashi, N. *J. Am. Chem. Soc.* **1998**, *120*, 3152.

(57) Esteruelas, M. A.; Werner, H. *Organomet. Chem.* **1986**, *303* (2), 221.

(58) Parr, R. G.; Yang, W. *Density-functional theory of atoms and molecules*; Oxford University Press: Oxford, 1989.

(59) Perdew, J. P.; Burke, K.; Ernzerhof, M. *Phys. Rev. Lett.* **1996**, *77*, 3865.

(60) Laikov, D. N. *Chem. Phys. Lett.* **1997**, *281*, 151.

(61) Ustynyuk, Y. A.; Ustynyuk, L. Y.; Laikov, D. N.; Lunin, V. V. *J. Organomet. Chem.* **2000**, *597*, 182.

(62) Cundari, T. R.; Stevens, W. J. *J. Chem. Phys.* **1993**, *98*, 5555.

(63) Stevens, W. J.; Basch, H.; Krauss, M. *J. Chem. Phys.* **1984**, *81*, 6026.

(64) Stevens, W. J.; Basch, H.; Krauss, M.; Jasien, P. *Can. J. Chem.* **1992**, *70*, 612.



$(\text{CO})(\text{P}^i\text{Pr}_3)_2$ .  $^1\text{H}$  NMR ( $\text{C}_6\text{D}_6$ , 20 °C), ppm: 1.12 (br m, 36H,  $\text{PCH}_3$ ), 2.64 (br m, 6H,  $\text{PCH}$ ).  $^{31}\text{P}\{^1\text{H}\}$  NMR ( $\text{C}_6\text{D}_6$ , 20 °C): 49.6. IR ( $\text{C}_6\text{D}_6$ ),  $\text{cm}^{-1}$ :  $\nu$  1911 (CO), 1582 (NO). The crystalline sample of  $\text{Ru(NO)Cl(CO)(P}^i\text{Pr}_3)_2$  for X-ray structure determination was obtained by slow evaporation of a toluene solution.

**Variable-Temperature Reaction of  $\text{RuHCl(CO)(P}^i\text{Pr}_3)_2$  with a Deficiency of NO.** A solution of 16 mg (0.033 mmol)  $\text{RuHCl(CO)(P}^i\text{Pr}_3)_2$  in 0.5 mL  $\text{C}_7\text{D}_8$  was placed in an NMR tube fitted with Teflon stopcock. The solution was freeze–pump–thaw–degassed 3 times in liquid  $\text{N}_2$ , the headspace was evacuated over the frozen solution, and 150 mm NO (0.02 mmol) was introduced into the tube. Then the solution was thawed, stirred briefly, and inserted into a precooled NMR probe.  $^1\text{H}$  and  $^{31}\text{P}\{^1\text{H}\}$  NMR at –60 °C showed 8% conversion of  $\text{RuHCl(CO)(P}^i\text{Pr}_3)_2$  to  $\text{Ru(NO)Cl(CO)(P}^i\text{Pr}_3)_2$  and 2% conversion to  $\text{RuH(HNO)Cl(CO)(P}^i\text{Pr}_3)_2$ . Data follow for –60 °C.  $^1\text{H}$  NMR ( $\text{C}_7\text{D}_8$ ), ppm: 1.20 (br m,  $\text{PCH}_3$ ), 2.43 (br m,  $\text{PCH}$ ), –24.35 (br s,  $\text{RuHCl(CO)(P}^i\text{Pr}_3)_2$ ), –7.65 (br,  $\text{RuH(HNO)Cl(CO)(P}^i\text{Pr}_3)_2$ ), 20.95 (br,  $\text{RuHNO}$ ).  $^{31}\text{P}\{^1\text{H}\}$  NMR ( $\text{C}_7\text{D}_8$ ), ppm: 48.5 (8%, s,  $\text{Ru(NO)Cl(CO)(P}^i\text{Pr}_3)_2$ ), 57.1 (90%, br s,  $\text{RuHCl(CO)(P}^i\text{Pr}_3)_2$ ), 61.5 (2%, br s,  $\text{RuH(HNO)Cl(CO)(P}^i\text{Pr}_3)_2$ ). Data follow for –40 °C.  $^1\text{H}$  NMR ( $\text{C}_7\text{D}_8$ ), ppm: 1.25 (br m,  $\text{PCH}_3$ ), 2.50 (br m,  $\text{PCH}$ ), –24.22 (br s,  $\text{RuHCl(CO)(P}^i\text{Pr}_3)_2$ ), –7.70 (td,  $J_{\text{PH}} = 23.0$  Hz,  $J_{\text{HH}} = 9.8$  Hz)  $\text{RuH(HNO)Cl(CO)(P}^i\text{Pr}_3)_2$ , 20.95 (d,  $J_{\text{HH}} = 9.8$  Hz,  $\text{RuHNO}$ ).  $^{31}\text{P}\{^1\text{H}\}$  NMR ( $\text{C}_7\text{D}_8$ ), ppm: 49.0 (14%, s,  $\text{Ru(NO)Cl(CO)(P}^i\text{Pr}_3)_2$ ), 57.6 (84%, br s,  $\text{RuHCl(CO)(P}^i\text{Pr}_3)_2$ ), 61.5 (2%, br s,  $\text{RuH(HNO)Cl(CO)(P}^i\text{Pr}_3)_2$ ). Upon warming to +20 °C, the  $^1\text{H}$  and  $^{31}\text{P}\{^1\text{H}\}$  peaks for the starting material are extremely broad and the only products that are present in the reaction mixture are  $\text{Ru(NO)Cl(CO)(P}^i\text{Pr}_3)_2$  and  $\text{RuH(HNO)Cl(CO)(P}^i\text{Pr}_3)_2$  in 1.5:1 ratio. IR of  $\text{RuH(HNO)Cl(CO)(P}^i\text{Pr}_3)_2$  ( $\text{C}_6\text{D}_6$ ),  $\text{cm}^{-1}$ :  $\nu$  1959 (CO), 1528 (NO). After 11 h at +23 °C,  $^{31}\text{P}\{^1\text{H}\}$  NMR shows  $\text{Ru(NO)Cl(CO)(P}^i\text{Pr}_3)_2$ ,  $\text{RuHCl(CO)(P}^i\text{Pr}_3)_2$ , and  $\text{RuH(HNO)Cl(CO)(P}^i\text{Pr}_3)_2$  in 4:1.4:1 ratio.

**Reaction of  $\text{RuHCl(CO)(P}^i\text{Pr}_3)_2$  with a Deficiency of NO in the Presence of 1,4-Cyclohexadiene.** A solution of 14.5 mg (0.030 mmol) of  $\text{RuHCl(CO)(P}^i\text{Pr}_3)_2$  and 55  $\mu\text{L}$  (0.6 mmol) of 1,4-cyclohexadiene in 0.5 mL of  $\text{C}_6\text{D}_6$  was placed in an NMR tube fitted with Teflon stopcock. The solution was frozen in liquid  $\text{N}_2$ , the headspace was evacuated, and 200 mm NO (0.02 mmol) was introduced into the tube. After stirring for 5 min at 23 °C,  $^1\text{H}$  and  $^{31}\text{P}\{^1\text{H}\}$  NMR showed complete conversion of  $\text{RuHCl(CO)(P}^i\text{Pr}_3)_2$  to a 1:1 mixture of  $\text{Ru(NO)Cl(CO)(P}^i\text{Pr}_3)_2$  and  $\text{RuH(HNO)Cl(CO)(P}^i\text{Pr}_3)_2$ . The same result is observed when  $\text{RuHCl(CO)(P}^i\text{Pr}_3)_2$  and NO are mixed in the same ratio in neat 1,4-cyclohexadiene.

**Variable-Temperature Reaction of  $\text{RuHCl(CO)(P}^i\text{Pr}_3)_2$  with Excess NO.** A solution of 16 mg (0.033 mmol) of  $\text{RuHCl(CO)(P}^i\text{Pr}_3)_2$  in 0.5 mL of  $\text{C}_7\text{D}_8$  was placed in an NMR tube fitted with Teflon stopcock. The solution was frozen in liquid  $\text{N}_2$ , the headspace was evacuated, and 760 mm NO (0.1 mmol) was introduced into the tube. Then the solution was thawed, stirred briefly, and inserted into a precooled NMR probe.  $^1\text{H}$  and  $^{31}\text{P}\{^1\text{H}\}$  NMR at –60 °C showed conversion of  $\text{RuHCl(CO)(P}^i\text{Pr}_3)_2$  to  $\text{Ru(NO)Cl(CO)(P}^i\text{Pr}_3)_2$  and  $\text{RuH(HNO)Cl(CO)(P}^i\text{Pr}_3)_2$  in a 31:1 product ratio. In addition to the signals corresponding to these two compounds,  $^1\text{H}$  NMR showed a broad peak at + 6.2 ppm attributed to HONO.

**EPR Monitoring of the Reaction of  $\text{RuHCl(CO)(P}^i\text{Pr}_3)_2$ .** EPR tubes were charged with solution of 16 mg (0.033 mmol) of  $\text{RuHCl(CO)(P}^i\text{Pr}_3)_2$  in 0.9 mL of  $\text{C}_7\text{H}_8$  and closed by a rubber septum. The solution was freeze–pump–thaw–degassed in liquid  $\text{N}_2$ , the headspace was evacuated, and 150–450 mm NO (0.02–0.06 mmol) was introduced into the tube. The solution was then thawed, stirred briefly, frozen in liquid  $\text{N}_2$ , and inserted into a precooled EPR probe. In an alternative mixing technique, NO was bubbled through the

solution cooled by an ethyl acetate/liquid  $\text{N}_2$  bath. The resulting EPR spectra were independent of the mixing technique. An identical procedure was followed with  $\text{RuDCl(CO)(P}^i\text{Pr}_3)_2$ . One of the EPR experiments showed, at earliest observation times, the presence of a radical different from  $\text{RuH(NO)(CO)Cl(P}^i\text{Pr}_3)_2$ . This first product was determined to be a Ru(III) product of oxidation of  $\text{RuHCl(CO)(P}^i\text{Pr}_3)_2$  by adventitious oxygen. This assignment was confirmed by observation of the identical EPR spectrum when a solution of  $\text{RuHCl(CO)(P}^i\text{Pr}_3)_2$  was contacted with air. In this case, the orange solution turns green, and the EPR spectrum resembles that reported in the literature for the Ru(III) product of a reaction of a Ru(II) complex with air.<sup>65</sup>

**Preparation of  $\text{RuDCl(CO)(P}^i\text{Pr}_3)_2$ .** A 0.1 g (0.2 mmol) portion of  $\text{RuHCl(CO)(P}^i\text{Pr}_3)_2$  was dissolved in 10 mL of benzene and placed in a 100 mL flask with a Teflon-coated stirbar. The solution was frozen in liquid  $\text{N}_2$ , the headspace evacuated, and 1 atm  $\text{D}_2$  added to headspace. After stirring for 12 h at +50 °C, the solvent was removed to give  $\text{RuDCl(CO)(P}^i\text{Pr}_3)_2$ . Yield: 0.1 g, 100%.  $^2\text{H}$  NMR for  $\text{RuDCl(CO)(P}^i\text{Pr}_3)_2$  ( $\text{C}_6\text{D}_6$ , 20 °C), ppm: –24.4 (br, Ru–D).

**Reaction of  $\text{RuDCl(CO)(P}^i\text{Pr}_3)_2$  with a Deficiency of NO.** A solution of 16 mg (0.033 mmol) of  $\text{RuHCl(CO)(P}^i\text{Pr}_3)_2$  in 0.9 mL of  $\text{C}_7\text{H}_8$  was placed in an EPR tube closed by a rubber septum. The solution was freeze–pump–thaw–degassed in liquid  $\text{N}_2$ , the headspace was evacuated, and 150 mm NO (0.02 mmol) was introduced into the tube. Then the solution was thawed, stirred briefly, frozen in liquid  $\text{N}_2$ , and inserted into a precooled EPR probe. In an alternative mixing technique, NO was bubbled through the solution cooled by an ethyl acetate/liquid  $\text{N}_2$  bath. The resulting EPR spectra were independent of the mixing technique. If  $\text{O}_2$  inadvertently contacts Ru(H or D)Cl(CO)(P<sup>i</sup>Pr<sub>3</sub>)<sub>2</sub> in solution, an EPR active species is produced; it shows signals at higher g value, which allows detection of the artifact.

**Reaction of  $\text{RuHCl(CO)(P}^i\text{Pr}_2(3,5\text{-(CF}_3)_2\text{C}_6\text{H}_3)_2$  with NO.** A solution of 18.6 mg (0.025 mmol) of  $\text{RuHCl(CO)(P}^i\text{Pr}_2(3,5\text{-(CF}_3)_2\text{C}_6\text{H}_3)_2$  in 0.5 mL of  $\text{C}_6\text{D}_6$  was placed in an NMR tube fitted with a Teflon stopcock. The solution was freeze–pump–thaw–degassed 3 times in liquid  $\text{N}_2$ , the headspace above the frozen solution was evacuated, and 150 mm atm NO (0.020 mmol) was introduced into the tube. The color of the solution turned red from yellow. After stirring for 10 min at 23 °C,  $^1\text{H}$  and  $^{31}\text{P}\{^1\text{H}\}$  NMR showed complete conversion of  $\text{RuHCl(CO)(P}^i\text{Pr}_2(3,5\text{-(CF}_3)_2\text{C}_6\text{H}_3)_2$  to a mixture of  $\text{RuHCl(HNO)(CO)(P}^i\text{Pr}_2(3,5\text{-(CF}_3)_2\text{C}_6\text{H}_3)_2$  and  $\text{RuCl(NO)(CO)(P}^i\text{Pr}_2(3,5\text{-(CF}_3)_2\text{C}_6\text{H}_3)_2$  in a 1:1 ratio.  $^1\text{H}$  NMR ( $\text{C}_6\text{D}_6$ , 20 °C), ppm: 7.96 (td,  $J_{\text{HP}} = 21.9$  Hz,  $J_{\text{HH}} = 9.6$  Hz,  $\text{RuH(HNO)}$ ), 0.5–1.15 (overlapping m,  $\text{PCH}_3$ ), 2.26, 2.49, 2.55, 3.01 (m,  $\text{PCH}$ ), 7.70 (s,  $p\text{-3,5-(CF}_3)_2\text{C}_6\text{H}_3$ ), 8.08, 8.17 ( $o\text{-3,5-(CF}_3)_2\text{C}_6\text{H}_3$ ), 21.23 (d,  $J_{\text{HH}} = 9.6$  Hz,  $\text{Ru(HNO)}$ ).  $^{31}\text{P}\{^1\text{H}\}$  NMR ( $\text{C}_6\text{D}_6$ , 20 °C): 49.9 (s,  $\text{RuCl(NO)(CO)(P}^i\text{Pr}_2(3,5\text{-(CF}_3)_2\text{C}_6\text{H}_3)_2$ ), 63.3 (s,  $\text{RuHCl(HNO)(CO)(P}^i\text{Pr}_2(3,5\text{-(CF}_3)_2\text{C}_6\text{H}_3)_2$ ).

**Crystal Structure Determination of  $\text{RuCl(NO)(CO)(P}^i\text{Pr}_3)_2$ .** An orange crystal (approximate dimensions 0.20 × 0.20 × 0.15 mm<sup>3</sup>) was placed onto the tip of a 0.1 mm diameter glass capillary and mounted on a SMART6000 (Bruker) at 120(2) K. A preliminary set of cell constants was calculated from reflections harvested from three sets of 20 frames. These initial sets of frames were oriented such that orthogonal wedges of reciprocal space were surveyed. This produced initial orientation matrices determined from 341 reflections. The data collection was carried out using Mo K $\alpha$  radiation (graphite monochromator) with a frame time of 7 s and

(65) James, B. R.; Mikkelsen, S. R.; Leung, T. W.; Williams, G. M.; Wong, R. *Inorg. Chim. Acta* **1984**, 85, 209.

a detector distance of 5 cm. A randomly oriented region of reciprocal space was surveyed to the extent of 1.2 spheres and to a resolution of 0.51 Å. Five major sections of frames were collected with 0.30° steps in  $\omega$  at 5 different  $\phi$  settings and a detector position of  $-43^\circ$  in  $2\theta$ . An additional set of 50 frames was collected in order to model decay. The intensity data were corrected for absorption.<sup>66</sup> Final cell constants were calculated from the  $xyz$  centroids of 8152 strong reflections from the actual data collection after integration (SAINT).<sup>67</sup> The space group  $C2/c$  was determined on the basis of systematic absences and intensity statistics. The structure was solved using SHELXS-97 and refined using SHELXL-97.<sup>68</sup> A Patterson solution was calculated which provided the position of the heavy atoms. Full-matrix least-squares/difference Fourier cycles were performed which located the remaining atoms. All non-hydrogen atoms were refined with anisotropic displacement parameters. All hydrogen atoms were placed in ideal positions and refined as riding atoms with individual isotropic displacement parameters. The ruthenium and nitrogen atom are located on a 2-fold axis, and the oxygen atom of the nitrosyl group is disordered over two positions (50:50). Likewise, the chlorine atom and the carbonyl moiety are disordered with each other (50:50). Ruthenium is located 0.45 Å above the basal plane (least squares calculated from C11, C11a, P1, P1a). The residual electron density is located in the vicinity of heavy atoms and on bonds.

**NMR Tube Reaction of OsHCl(CO)(P<sup>i</sup>Pr<sub>3</sub>)<sub>2</sub> with NO.** A solution of 14 mg (0.021 mmol) of OsHCl(CO)(P<sup>i</sup>Pr<sub>3</sub>)<sub>2</sub> in 0.5 mL of C<sub>6</sub>D<sub>6</sub> was placed in an NMR tube fitted with Teflon stopcock. The solution was freeze–pump–thaw–degassed 3 times in liquid N<sub>2</sub>, the headspace above the frozen solution was evacuated, and 80 mm NO (0.011 mmol) was introduced into the tube. After stirring for 10 min at 23 °C, <sup>31</sup>P{<sup>1</sup>H} NMR showed the absence of signals for starting material and any products; <sup>1</sup>H NMR showed the

disappearance of the hydride signal of the starting material at  $-32.5$  ppm, as well as a significant decrease in intensity for the alkyl signals of the phosphine ligands. A new broad signal was observed at 4.00 ppm and attributed to HONO. After the additional 760 mm NO (0.1 mmol) was introduced, the color of the reaction mixture turned orange. After 10 min stirring at 23 °C, <sup>31</sup>P{<sup>1</sup>H} NMR showed the presence of OsCl(NO)(CO)(P<sup>i</sup>Pr<sub>3</sub>)<sub>2</sub> (25.3 ppm) and OsHCl(HNO)(CO)(P<sup>i</sup>Pr<sub>3</sub>)<sub>2</sub> (34.2 ppm) in 4.4:1 ratio. <sup>1</sup>H NMR (C<sub>6</sub>D<sub>6</sub>), ppm:  $-8.37$  (td,  $J_{\text{PH}} = 25.1$  Hz,  $J_{\text{HH}} = 8.8$  Hz, OsH(HNO)Cl(CO)(P<sup>i</sup>Pr<sub>3</sub>)<sub>2</sub>), 0.9–1.2 (m, PCH<sub>3</sub>), 2.60 (m, PCH), 3.98 (br, HONO), 21.90 (d,  $J_{\text{HH}} = 8.8$  Hz, OsHNO). After 18 h of stirring at 23 °C, <sup>31</sup>P{<sup>1</sup>H} NMR indicated that the OsCl(NO)(CO)(P<sup>i</sup>Pr<sub>3</sub>)<sub>2</sub>/OsHCl(HNO)(CO)(P<sup>i</sup>Pr<sub>3</sub>)<sub>2</sub> ratio changed to 22:1.

**ReactIR-Monitored Reaction of OsHCl(CO)(P<sup>i</sup>Pr<sub>3</sub>)<sub>2</sub> with NO.**

A solution of 50 mg (0.075 mmol) of OsHCl(CO)(P<sup>i</sup>Pr<sub>3</sub>)<sub>2</sub> in 3 mL of C<sub>6</sub>H<sub>6</sub> was placed in a ReactIR flask. A 1.2 mL portion of NO (0.05 mmol) at 1 atm was slowly bubbled through the solution using a needle and a gastight syringe. The IR difference spectra (relative to OsHCl(CO)(P<sup>i</sup>Pr<sub>3</sub>)<sub>2</sub> solution) taken during 2 h showed a gradual decrease for  $\nu(\text{CO})$  of starting material (1888 cm<sup>-1</sup>) and the growth of two new peaks at 1903 and 1559 cm<sup>-1</sup>, corresponding to  $\nu(\text{CO})$  and  $\nu(\text{NO})$  of OsH(NO)Cl(CO)(P<sup>i</sup>Pr<sub>3</sub>)<sub>2</sub>. After an additional 1.2 mL of NO was bubbled through the reaction mixture, the IR difference spectrum showed the growth of new peaks at 1929 and 1388 cm<sup>-1</sup>, corresponding to  $\nu(\text{CO})$  and  $\nu(\text{NO})$  of OsH(HNO)Cl(CO)(P<sup>i</sup>Pr<sub>3</sub>)<sub>2</sub>, and at 1892 and 1552 cm<sup>-1</sup>, corresponding to  $\nu(\text{CO})$  and  $\nu(\text{NO})$  of Os(NO)Cl(CO)(P<sup>i</sup>Pr<sub>3</sub>)<sub>2</sub>.

**Acknowledgment.** This work was supported by the Department of Energy. We also thank Prof. P. A. Evans for use of his React-IR equipment.

**Supporting Information Available:** Full crystallographic data (CIF). This material is available free of charge via the Internet at <http://pubs.acs.org>.

IC0349407

(66) Blessing, R. *Acta Crystallogr.* **1995**, 33.

(67) SAINT 6.1; Bruker Analytical X-ray Systems: Madison, WI.

(68) SHELXTL-Plus V5.10; Bruker Analytical X-ray Systems: Madison, WI.